# Depth inversion for nonlinear waves shoaling over a barred-beach

Stéphan T. Grilli [1], M. ASCE, and Jesper Skourup [2]

**ABSTRACT :** Characteristics of periodic wave shoaling over a barred-beach are calculated in a fully nonlinear numerical wave tank. Variations of wave elevation, slopes, height, asymmetry, and celerity are discussed. Over and beyond the bar, classical highly nonlinear decomposition phenomena occur in a *modulation region* (MR); in shallower water, shoaling reoccurs. Depth inversion algorithms developed and calibrated for mild slopes are applied to the barred-beach. Expectedly, errors on depth prediction occur in the MR; suggestions for improvements are made.

## INTRODUCTION

### Depth inversion algorithms

Depth inversion refers to a class of numerical/experimental methods by which the ocean bottom bathymetry in coastal areas is predicted using properties of waves measured on the ocean surface. Such properties are typically obtained by remote sensing or video based technique [see Grilli, 1998, for a brief summary of these] and often consist, in their raw form, in spatial and temporal variations of wave phases. Multiple phase diagrams separated in time can provide estimates of wave celerity and wavelength [hence, wave period] which, in turn, using a dispersion relationship, can provide estimates of the depth variation. Both the quality of the initial data and the accuracy of the dispersion relationship in representing real wave behavior will affect the accuracy of the depth prediction.

Most state-of-the-art methods still use the linear dispersion relationship to carry out depth inversion, according to the methodology outlined above [Dugan,

[1]Distinguished Professor, *Dept. of Ocean Engng., University of Rhode Island, Narragansett, RI 02882, USA*, email: grilli@oce.uri.edu, http://www.oce.uri.edu/~grilli

[2]*Danish Hydraulic Institute, Agern Allé 5, Horsholm DK 2970, Denmark*, email : jes@dhi.dk

1997]. Grilli (1998), however, studied the depth inversion problem for mildly and monotonously sloping beaches and showed, for shallow enough water, nonlinear effects and their influence on wave celerity $c$ cannot be neglected. Such so-called *amplitude dispersion effects* make higher waves travel faster and lead to overestimation of the water depth $h$, when depth inversion is simply the result of "inverting" the linear dispersion relation. To account for amplitude dispersion effects, wave height data $H$ or, at least, deep water steepness $k_oH_o$ must also be known [$k_o$ and $H_o$ are the deep water wavenumber and wave height, respectively]. For periodic waves, normalized wave steepness $kH/k_oH_o$ was shown by Grilli and Horrillo (1996,1998b) to provide an almost one-to-one relationship with relative depth $kh$ in the shoaling region and, also [surprisingly], to be well predicted by linear wave theory (LWT). Hence, assuming simultaneous observations of surface elevations are available, they suggested that this parameter could be used to model the wave height variation, and thus predict $k_oH_o$, in the *depth-inversion problem.*

Following this approach, assuming both wave phases and wave height data are available, Grilli (1998) developed a new *Depth Inversion Algorithm* [referred to as DIA1] and validated it for simulated wave data. This algorithm uses a dispersion relation $c(k_oh, k_oH_o)$ which is empirically based on results of computations in a fully nonlinear wave tank [NWT; see next Section]. In all cases, rms-errors on depth inversion with DIA1 were less than a few percent whereas the linear dispersion led to rms-errors 5 to 10 times larger, particularly in the shallower water region. Accurate spatial measurements of wave elevations, for instance using remote sensing techniques such as Synthetic Aperture Radar (SAR), are still quite problematic under the current state of the technology. Hence, to eliminate the need for wave height data, an alternate parameter related to wave skewness, also function of $k_oH_o$, was identified and shown to be quite sensitive to depth variations (Grilli and Horrillo, 1996,1998b). This parameter is the ratio of forward to backward wave slopes, noted, $s_2/s_1 \simeq L_1/L_2$ [Fig. 1b, assuming $H_1 \simeq H_2$; i.e., a measure of wave left to right spatial asymmetry]. Unlike $H$, this parameter can also be retrieved from spatial wave phase information. Thus, Grilli (1998) developed a second algorithm [referred to as DIA2], using an empirical relationship $s_2/s_1(k_oh, k_oH_o)$, also fitted to results of computations in the NWT, to predict $k_oH_o$ before the nonlinear dispersion relation is "inverted" to predict depth. Although DIA2 provided slightly larger errors on depth prediction than DIA1, these were still much smaller than when using LWT.

In actual field situations, DIA1 and DIA2 would thus predict the depth variation $h(x)$ in the direction of wave propagation, for waves almost normally incident to the shore [i.e., about cross-shore], based on sets of values of $c(x)$ and $L(x)$ [obtainable from wave phases], and either $H(x)$ (DIA1) or $s_2/s_1(x)$ (DIA2), simultaneously measured at a number of locations $x$, using remote sensing techniques (Fig. 1). In both algorithms, wave period $T$ is first predicted as the mean of observed $L/c$ values [where $L = (L_c(x) + L_t(x))/2$; Fig. 1b], and $k_oH_o$ is then predicted [with, $k_o = (2\pi)^2/(gT^2)$], either based on wave height data, using the LWT steepness

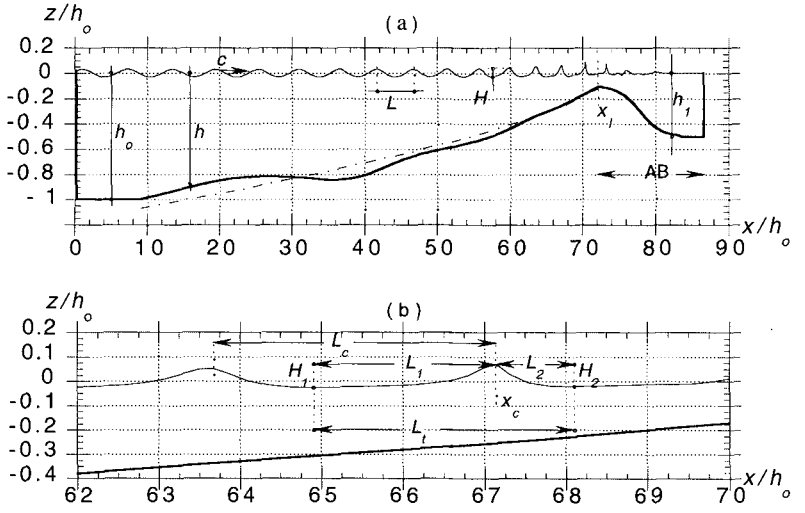


Figure 1: (a) Sketch of periodic wave shoaling computations in the *numerical wave tank*. (——) typical bottom topography and (— - —) least square fit to the topography : $h/h_o = 0.0758\,(74.20 - x/h_o)^{0.64}$ (Dean's profile). (b) Blow-up of part (a) and definition of some of the wave geometric characteristics used in DIA1 and DIA2.

relationship (DIA1), or on wave asymmetry data, using the empirical relationship for $s_2/s_1(k_o h, k_o H_o)$ (DIA2). The celerity relationship $c(k_o h, k_o H_o)$ is finally inverted to predict depth $h$ [see details in Grilli, 1998].

## Computation of wave shoaling in a numerical wave tank

Nonlinear properties of periodic waves of height $H_o$ and period $T$ in deep water, shoaling over "cylindrical beaches" with *monotonously decreasing and mildly sloping* depth variation $h(x)$ (Fig. 1), were used by Grilli (1998) to calibrate depth inversion algorithms DIA1 and DIA2.

These properties were obtained by Grilli and Horrillo (1996,1998b), using a two-dimensional (2D) *numerical wave tank* (NWT), which combined [Grilli et al., 1989; Grilli and Subramanya, 1996; Grilli and Horrillo, 1997; Fig. 2a] : (i) a higher-order Boundary Element (BEM) solution of Fully Nonlinear Potential Flow (FNPF) equations in domain $\Omega$; (ii) an exact generation of finite amplitude periodic waves [*Streamfunction Waves*] at the deeper water extremity ($\Gamma_{r1}$); and (iii) an *Absorbing Beach* (AB) at the far end of the tank [featuring both free surface absorption on $\Gamma_f$

and lateral active absorption (AP) on $\Gamma_{r2}$; Clément, 1997]. A feedback procedure was developed to adaptively calibrate the beach absorption coefficient so as to absorb the period-averaged energy of waves entering the AB at $x = x_l$. After absorption of initial transient waves, computations in the NWT reached a *quasi-steady* state for which reflection from the AB was very small. Nonlinear properties of waves were then calculated and validation tests were performed to assess their sensitivity to the AB location and to the resolution of the spatial discretization. Numerical results were compared to laboratory experiments for periodic wave shoaling over a mild slope, and propagation over a bar [Beji and Battjes, 1994]. All the tests were found satisfactory. Details of model equations, numerical methods and validation applications can be found in the above-referenced papers.

Grilli and Horrillo (1996,1998b) calculated shoaling of waves of various heights and periods up to very close to the breaking point, over 1:35, 1:50, and 1:70 slopes, both plane and natural [i.e., with a bathymetry following Dean's (1991) equilibrium beach profile; see, e.g., Fig. 1a]. Local [i.e., variations of shoaling coefficient $K_S = H/H_o$, celerity $c$, relative wave height $H/h$, steepness $kH$, and asymmetry $s_2/s_1$], and integral properties of shoaling waves were calculated. Due to the low reflection from the slope and the AB, wave properties were found to be very repeatable for successive waves.

For mild slopes, nonlinear properties of waves of different height and period but same deep water steepness $k_oH_o$ were found to be almost identical for the same relative depth $kh$. This allowed Grilli (1998) to use results for a plane 1:50 slope to calibrate DIAs which were later successfully applied to other slopes. In the shallower water region, linear, weakly nonlinear, and higher-order steady wave theories did not, in general, accurately predict shoaling wave properties, especially for $H/h > 0.15$. Linear wave theory, in particular, was in error by up to 85% for the wave celerity. The weak nonlinearity and/or the lack of wave skewness in these theories were identified as the main sources of errors.

## WAVE SHOALING OVER BARRED-BEACHES

### General features

Grilli and Horrillo (1998a) used the same NWT as above to calculate periodic wave shoaling over a barred-beach, modeled as a Dean's equilibrium profile with average slope 1:50 (Fig. 2), and a bar located towards the top of the slope, with a 1:20 seaward, a 1:10 shoreward slope, and a crest with nondimensional depth 0.2. [The geometry of this bar is similar to that of Beji and Battjes' (1994) experiments which were used to validate shoaling computations in the NWT.]

Since waves of moderate incident steepness initially behave as predicted by LWT, the computations are initiated in intermediate water depth $h_o^* = 0.6h_o$, in the de-shoaling zone. Corresponding wave characteristics in deep water (depth $h_o$) are back-calculated using LWT. Three incident waves of nondimensional height $H_o'^* =$

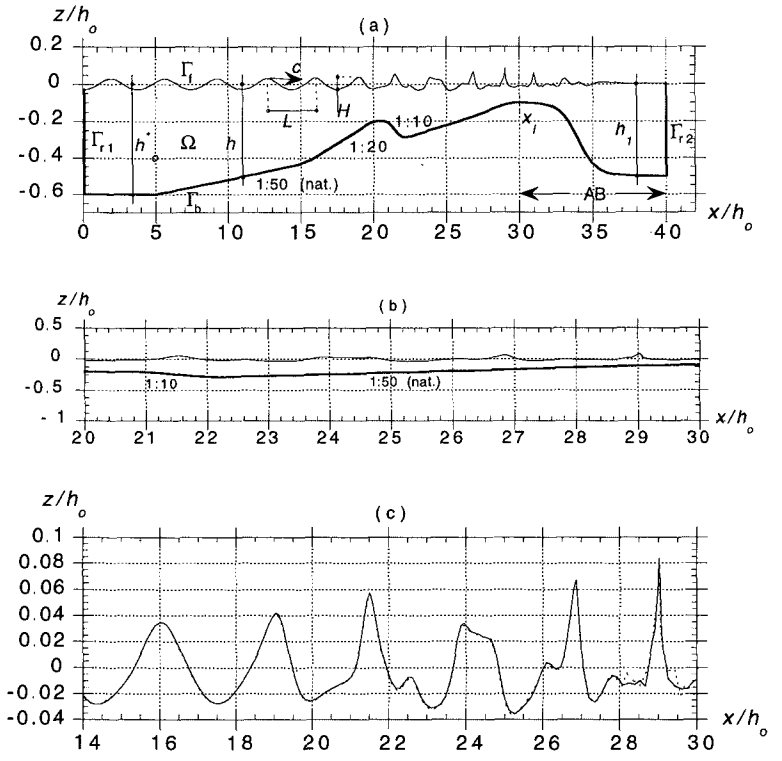


Figure 2: Periodic wave shoaling over a barred-beach. (a) Sketch of NWT. (b) Blow-up of free surface shape in undistorted scale. (c) Free surface shape for case 1 (Table 1) : after $15.75T'$ (——); one period later (- - - - -).

Table 1: Input characteristics of incident waves in the NWT : $H'_o$ deep water wave height; $T'$ wave period; $H'^*_o$ initial wave height in depth $h'^*_o = 0.6$; $k'_o = (2\pi/T')^2$ (linear) deep water wave number; $k_o H_o$ initial wave steepness; $c'_o = T'/(2\pi)$ and$L'_o = c'_o T$, the linear deep water wave celerity and wavelength, respectively. Dashes indicate nondimensional variables (length scale : $h_o$; time scale : $\sqrt{h_o/g}$, with $g$, the gravitational acceleration).

| No. | $H'_o$ | $T'$ | $H'^*_o$ | $k'_o$ | $k_o h^*_o$ | $k_o H_o$ |
|---|---|---|---|---|---|---|
| 1 | 0.0635 | 5.5 | 0.06 | 1.305 | 0.79 | 0.0852 |
| 2 | 0.0626 | 6.5 | 0.06 | 0.934 | 0.56 | 0.0594 |
| 3 | 0.0614 | 7.5 | 0.06 | 0.702 | 0.42 | 0.0361 |

$H^*_o/h_o = 0.06$ and periods $T' = T\sqrt{g/h_o} = 5.5$, 6.5, and 7.5 are successively generated at $\Gamma_{r1}$, as exact finite amplitude zero-mass-flux streamfunction waves (Grilli and Horrillo, 1997). General data for these three waves are summarized in Table 1. An AB is specified in the NWT for $x' \geq x'_l = 30$, with a tapered bottom variation aimed at improving energy absorption (Grilli and Horrillo, 1997); the depth at the AB entrance is $h'_l = 0.1$, and $h'_1 = 0.5$ at its extremity. Numerical data in the NWT [i.e., spatial and temporal discretizations] are selected for each case in order to ensure high accuracy of the computations.

A typical result for the calculated free surface shape is shown in Fig. 2, for case 1 (Table 1) at $t' = 86.64 = 15.75T'$ from the (cold) start of the computations. At this stage, the initial transient front has been absorbed in the AB and computations have reached a quasi-steady state. This is confirmed in Fig. 2c which shows two free surface profiles obtained at a one-period time interval : the two profiles are nearly identical, except for small high-frequency oscillations close to the AB entrance ($x' > 28$). Seaward of the bar ($x' \leq 21$), wave shoaling appears qualitatively similar to that obtained for monotonous mild slopes (e.g., Fig. 1) : as waves propagate up the beach, their length reduces, their height increases, and their profile becomes increasingly front/back asymmetric (i.e., skewed), with higher and narrower crests, and longer and shallower troughs. Shoreward of the bar ($x' \geq 21$), however, the free surface profile appears very different from typical shoaling profiles, and decomposes into higher-frequency oscillations. Such decomposition phenomena of waves propagating over obstacles are well known and have been observed, e.g, by Byrne (1969) and Young (1989), and modeled, e.g., by Massel (1983), Rey (1992), Rey et al (1992), Driscoll et al (1992), and Ohyama and Nadaoka (1994). Just before entering the AB, close to the breaking point ($x' \geq 28$), waves somewhat recover the sawtooth/soliton-like shape typical of pre-breaking shoaling waves.

Unlike in Driscoll et al's (1992) and Ohyama and Nadaoka's (1994) work, the present study features a varying beach topography. Hence, when waves reach the bar, due to the initial shoaling over the mildly sloping base-profile of the beach, they are

already significantly nonlinear with a height of about 45% of the local depth, and significant energy transferred to bound second and higher-order harmonics. Upon reaching the deeper water region behind the bar, wave nonlinearity drops and, as over a flat bottom, the higher harmonics are released as free waves. These free waves induce significant spatial modulations of the wave profile, quite apparent in Fig. 2, over some distance but, further onshore, as waves again propagate up the base-profile of the beach and depth decreases, shoaling reoccurs and, for sufficiently shallow depth, the free higher harmonics, again, become bound to the main wave and the wave profile reassumes a typical shoaling shape. Therefore, unlike with underwater obstacles over constant depth, the modulation region shoreward of the bar is limited in extension by the reducing depth, clearly, as a function of incident wavelength, bar berm geometry, and beach slope. In the case of Fig. 2, the modulation region covers a horizontal distance of about 5-6$h_o$.

**Detailed features**

Detailed variations of local wave parameters over the barred-beach are now presented and, more specifically, in the modulation region beyond the bar, where wave behavior is irregular. Fig. 3, parts a to d, shows normalized wave harmonics $a_i$ [$i = 1, 2, 3$], height $H$, slopes $s_1$ and $s_2$, and celerity $c$, respectively, calculated for case 2. [Since results for the three cases are qualitatively similar, only detailed results for case 2 are presented here.] Both the FNPF results for a 1:50 natural slope [i.e., the base-profile of the beach without the bar] and those predicted by LWT for the barred-beach, have been plotted. Fig. 4, parts a and c shows comparisons of normalized wave height and celerity, calculated for cases 1, 2, and 3, as a function of $k_o h$; and part b shows wave front/back asymmetry $s_2/s_1$ as a function of $x/h_o$.

In Fig. 3a, as mentioned before, standard wave shoaling occurs in front of the bar ($x' \leq 21$; Fig. 2), where wave energy is continuously transferred from the fundamental to bound higher-order harmonics [the initial slight increase in $a_1$ is due to reflection by the slope]. As a result, wave shape becomes increasingly skewed and sawtooth-like. Upon passing over the bar berm ($x' > 21$), waves reach the deeper water region beyond the bar and the harmonics are released as free waves. This results in marked oscillations in harmonic amplitudes and in strong spatial modulations of the wave profile. The modulation length for $a_2$ is approximately 5.6$h_o$, i.e., about twice the wavelength in the middle part of the modulation region. Waves reassume their sawtooth-like shoaling shape before entering the AB ($x' \geq 30$), and the harmonic amplitudes seem to come back to a prolongation of what they were before reaching the bar.

In Fig. 3b, similarly, the FNPF wave height variation for the barred-beach departs from that corresponding to the base-profile, upon reaching the bar berm. Towards the end of the modulation region beyond the bar, however, the barred-beach results seem to agree better with the latter. As expected from earlier studies, LWT

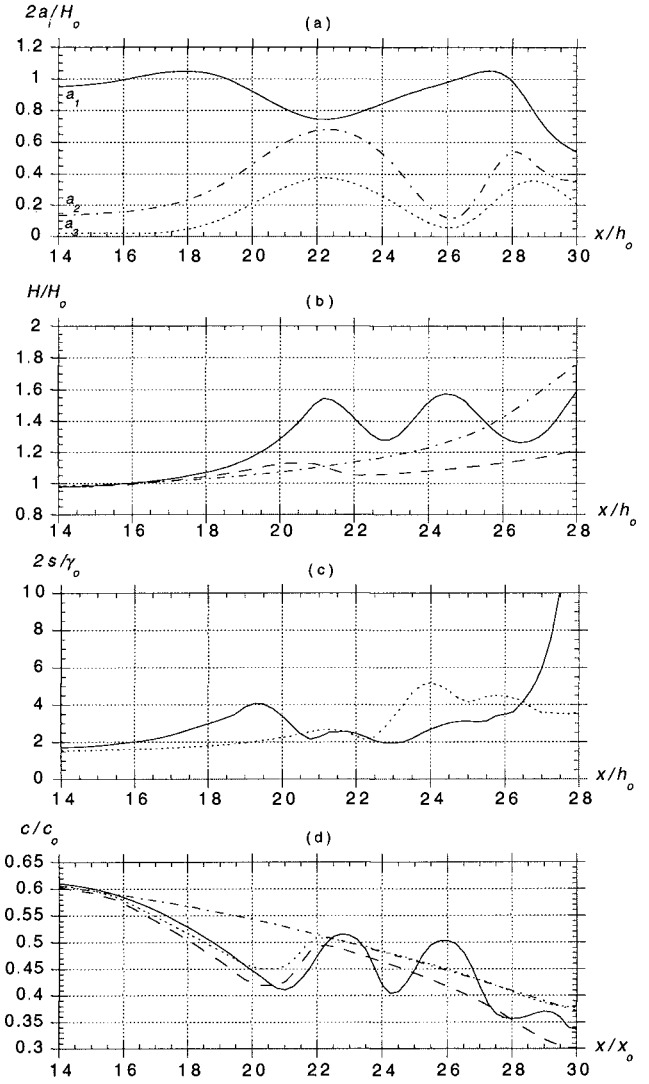


Figure 3: Normalized NWT results for case 2 (Table 1), over barred-beach of Fig. 2, compared with (– – –) LWT results for the same case; (- - -) NWT computations for the natural 1:50 base-profile (without a bar) : (a) First three wave harmonic amplitudes $a_i$. (b) Wave height (——). (c) Front (——) ($s_2 = H_2/L_2$) and back (- - - -) ($s_1 = H_1/L_1$) wave slopes ($\gamma_o = H_o/L_o$). (d) Wave celerity (——); (- - - -) application of based-profile results to the barred-beach.

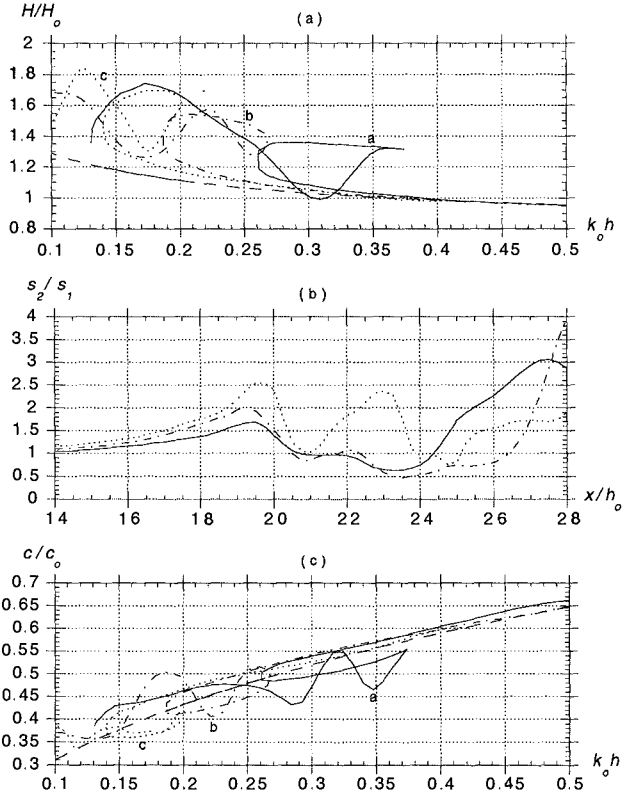


Figure 4: Normalized NWT results as a function of $k_o h$ for cases : (——; a) 1; (– – –; b) 2; and (- - - -; c) 3 in Table 1; and (– – –) indicates LWT results. (a) Wave height. (b) front/back asymmetry. (d) Wave celerity.

significantly underpredicts wave height. In Fig. 4a, due to wave modulations, the FNPF height variations for the barred-beach are multiple-valued functions of relative depth $k_o h$ [whereas LWT gives superimposed single-valued results; this would also be the case for results of the base-profile]. The patterns of wave height variations beyond the bar in the three cases show clear similarities.

In Fig. 3c, prior to reaching the bar, both front and back wave slopes, $s_2 = H_2/L_2$ and $s_1 = H_1/L_1$, continuously increase due to shoaling, with a larger relative increase for the front slope than for the back slope, due to increasing wave skewness. As a result, the front/back asymmetry $s_2/s_1$ in Fig. 4b, also continuously increases before the bar, from a value of 1 in deep water. For the beach base-profile, Grilli and Horrillo (1996,1998b) showed that this pattern is maintained up to reaching the AB. On the barred-beach, however, the modulations in wave shape beyond the bar induce significant changes in wave slopes. In each case, the wave front slope first reaches a maximum at around $x' = 19$, then drops over the bar berm and stabilizes beyond the bar, to finally increase again. The back slope keeps increasing over and beyond the berm and reaches a maximum at about 4.3 $h_o$ after the front slope reaches its maximum; the back slope then drops until $x' = 25$ [where water depth is about equal to the bar berm depth] and then stabilizes. In Fig. 4b, except for a backward shift in space of $1.5h_o$ or so, equal to the berm width, wave front/back asymmetry seems to correlate well in all cases, with the variations of $H/H_o$, such as in Fig. 3b for case 2, in the spatial region over and beyond the bar.

In Fig. 3d, the FNPF wave celerity variation for the barred-beach departs from that corresponding to the base-profile upon reaching the bar seaward slope. When corrected for depth, however, the latter results stay accurate until reaching the bar berm at $x' = 20$. This is because the 1:20 seaward slope is mild enough for the FNPF results, calculated for the same depth on the 1:50 natural slope, to apply in the present case. As expected, LWT underpredicts celerity before reaching the bar berm [and increasingly so, the longer the wave]. Celerity increases over and beyond the bar, as a result of the increasing depth, and then strongly oscillates in the modulation region, due to changes in wave height inducing amplitude dispersion effects for the celerity. Finally, just before reaching the AB, wave celerity seems to stabilize and agree better with the FNPF results calculated for the base-profile without the bar. As expected, FNPF results calculated for the base-profile and corrected for depth do not capture the celerity oscillations in the modulation region. They also overpredict celerity over the bar berm. This is also the case for LWT. In Fig. 4c, due to wave modulations, the FNPF celerity variations calculated for the barred-beach, for each case, are multiple-valued functions of relative depth $k_o h$ [whereas LWT gives superimposed single-valued results; this would also be the case for results of the base-profile corrected for depth]. Similarly to wave height, the patterns of wave celerity variations beyond the bar show clear similarities in the three cases.

The results for wave shape and celerity variations over and beyond the bar show that highly nonlinear phenomena of wave decomposition, harmonic generation,

and nonlinear exchanges of energy between harmonics occur and strongly affect the variation of wave parameters, as compared to the case without a bar. A further confirmation of the strong nonlinearity is given by calculating the typical nonlinearity parameters, $\delta = H/h$ and $\varepsilon = kH/2$, as a function of $x$. Due to shoaling, in all cases, the wave height to depth ratio $\delta$ already reaches a large 45 to 50% value over the bar, then drops beyond the bar, due to the increasing depth. For $x' > 25$, as shoaling re-occurs, $\delta$ starts increasing again, to eventually reach $\mathcal{O}(1)$ values or more, before waves enter the AB. Similarly, wave steepness, $\varepsilon$, keeps increasing due to shoaling up to reaching a large 0.10 to 0.12 value at the bar; it then oscillates beyond the bar to finally increase again up to 0.12 to 0.17 [for comparison, the deep water steepness of the limiting Stokes wave is $\varepsilon_{ol} = 0.44$].

## DEPTH INVERSION OVER BARRED-BEACHES

Results presented in the previous Section for periodic wave shoaling over a barred-beach show how local properties of waves such as $H/H_o$, $s_2/s_1$ and $c/c_o$, differ from the results obtained by Grilli and Horrillo (1996,1998b) for monotonously decreasing mild slopes. Differences mostly occur in the region over and at the lee side of the bar, the so-called *wave modulation region*. As variations of local wave properties with $k_o h$ and $k_o H_o$ are the bases for the depth inversion algorithms DIA1 and DIA2 proposed by Grilli (1998), it is expected that these algorithms will perform poorly to retrieve depth over and directly beyond the bar.

To confirm this prediction, DIA1 was applied to the results of cases 1, 2, and 3 in Table 1. To be fair, the wave height data used to estimate $k_o H_o$ in the algorithm, and the wavelength data used to estimate $T$, were limited to the monotonously varying region before the bar-berm, over the 1:50 natural base-profile and the 1:20 seaward slope of the berm [for $x' < 20$]. In a real field case, this monotonous part of the data could easily be identified. The corresponding direct prediction of both $H$ [and thus $k_o H_o$] and $T$ gave $R^2$ values of better than 99.3%. Depth was then retrieved using the celerity computed over the whole barred-beach, by inverting the FNPF celerity predicted on a mild slope for the same incident wave steepness and relative depth [i.e., such as the one plotted in Fig. 3d as curve (- - - -)]. Fig. 5, parts a to c, shows the results of this depth inversion for cases 1 to 3 in Table 1, compared to the actual depth variation and to the prediction of LWT. As expected, before the bar, for $x' < 20$, DIA1 gives quite a good prediction of depth whereas LWT overpredicts depth. Beyond the bar, however, both DIA1 and LWT fail to model the oscillatory behavior of wave celerity (Fig. 3d) and, hence, instead, wrongly predict an oscillatory bottom topography within the wave modulation region. In fact, as wave nonlinearity initially decreases in this region, thus reducing amplitude dispersion effects on the celerity, LWT does a somewhat better job in locating both the berm depth and the shape of the shoreward side of the berm. Beyond the modulation region [$x' \geq 28$], as shoaling more or less re-occurs as would be expected over the base-profile, the depth prediction in DIA1 improves while LWT again overpredicts depth.

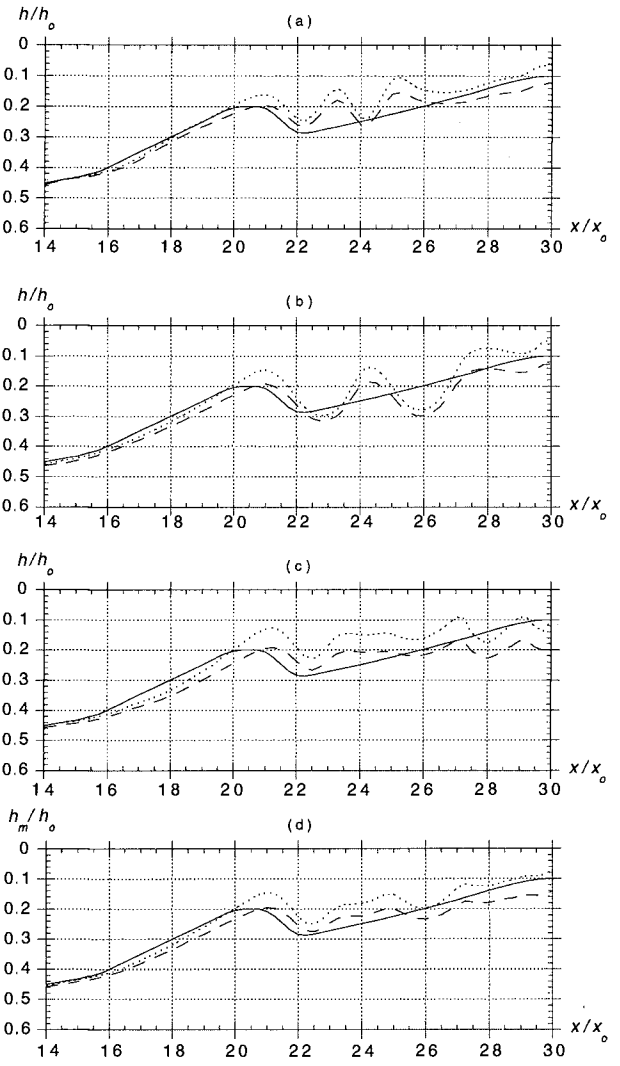


Figure 5: Depth inversion for the barred-beach and cases [Table 1] : (a) 1; (b) 2; and (c) 3. (——) Actual depth variation; (– – –) prediction by inversion of LWT dispersion relation; (- - - -) prediction by application of DIA1.(d) mean of results of the three cases in parts a-c.

In Fig. 5d, the depth predictions for the three cases have been averaged which, due to both different modulation regions and amplitudes of oscillations, somewhat limits the effects of wave decomposition on depth prediction. We thus see that DIA1 provides a good depth prediction for $x' \leq 20$ and $x' > 28$. In between, in the modulation region, depth is underpredicted by DIA1 and, as explained above, LWT does a somewhat better job in predicting depth.

## CONCLUSIONS

Shoaling of three periodic waves was calculated over a barred-beach in a two-dimensional fully nonlinear NWT. Results showed that : (i) prior to reaching the bar berm, wave shoaling occurs as over mild slopes; (ii) for waves with large non-linearity over the bar [such as here with $H/h = 0.45 - 0.50$], the increasing depth beyond the bar induces highly-nonlinear *wave decomposition* phenomena, with energy transfer between harmonics and the release of bound higher-harmonics into free waves; (iii) a *modulation region* appears beyond the bar, with a spatial extension function of the incident wave period/length, in which wave parameters such as celerity $c$, height $H$, and asymmetry $s_2/s_1$, become strongly oscillatory; (iv) repetitive patterns of variations of wave *front and back slope* occur in the modulation region; these could be used to locate the berm and predict the extension of the modulation region in DIAs; (v) as *shoaling re-occurs* beyond the modulation region, waves eventually reassume a shape and behavior similar to that observed over mildly sloping beaches; and (vi) since variations of local wave properties over mild slopes are the bases for the earlier depth inversion studies (Grilli, 1998), DIA1, expectedly, performs poorly within the modulation region; its performance is good otherwise.

For DIA1 to perform better in the modulation region, wave parameters would have to be analyzed and parameterized in the algorithm, based on the present and other similar computations of wave characteristics over barred-beaches. This is the object of future extensions to this work.

## Acknowledgments

This publication, in part, is based on research sponsored by the US Naval Research Laboratory, Stennis Space Center, grants N-00014-95-1-G607 and N-00014-96-C012, from the Remote Sensing Division (code 7240).

## References

Beji, S. and Battjes, J.A., Experimental investigation of wave propagation over a bar. *Coastal Engng.*, **23**, 1-16, 1994.

Byrne, R.J., Field occurrences of induced multiple gravity waves. *J. Geophys. Res.*, **74**, 2590-2596, 1969.

Clément, A., Coupling of two absorbing boundary conditions for 2D time-domain simulations of free surface gravity waves. *J. Comp. Phys.*, **126**, 139-151, 1996.

Dean, R.G., Equilibrium beach profiles : characteristics and applications. *J. Coastal Res.*, **7**(1), 53-84, 1991.

Driscoll, A.M., Dalrymple, R.A. and Grilli, S.T., Harmonic generation and transmission past a submerged rectangular obstacle. In *Proc. 23rd Intl. Conf. on Coastal Engineering* (Venice, Italy), Vol 1, pp 1142-1152. ASCE edition, 1992.

Dugan, J., Bathymetry measurements from long range airborne imaging systems. *Proc. 4th Intl. Conf. on Remote Sensing for Marine and Coastal Environments*, Orlando, Florida, 1997.

Grilli, S.T., Depth inversion in shallow water based on nonlinear properties of shoaling periodic waves. *Coastal Engineering* (in press), 1998.

Grilli, S.T. and Horrillo, J., Fully nonlinear properties of periodic waves shoaling over slopes. In *Proc. 25th Intl. Conf. on Coastal Engineering* (Orlando, Florida), Vol 1, pp 717-730. ASCE edition, 1996.

Grilli, S.T. and Horrillo, J., Numerical generation and absorption of fully nonlinear periodic waves. *J. Engng. Mech.*, **123**(10), 1060-1069, 1997.

Grilli, S.T. and Horrillo, J., Computation of periodic wave shoaling over barred-beaches in a fully nonlinear numerical wave tank. In Proc. ISOPE98 (Montreal, Canada, May 1998) (eds. Chung, J.S., Olagnon, M., Kim, C.H., Koterayama, W.), Vol 3, pp 294-300, 1998a.

Grilli, S.T. and Horrillo, J., Nonlinear properties of periodic waves shoaling over mild slopes. Submitted to *J. Geophys. Res.*, 1998b.

Grilli, S., Skourup, J., and Svendsen, I.A., An efficient boundary element method for nonlinear water waves, *Engng. Analysis with Boundary Elements*, **6**(2), 97-107, 1989.

Grilli, S.T. and Subramanya, R., Numerical modeling of wave breaking induced by fixed or moving boundaries. *Computational Mech.*, **17**, 374-391, 1996.

Massel, S.R., Harmonic generation by waves propagating over a submerged step. *Coastal Engng.*, **7**, 357-380, 1983.

Ohyama, T. and Nadaoka, K., Transformation of a nonlinear wave train passing over a submerged shelf without breaking. *Coastal Engng.*, **24**, 1-22, 1994.

Rey, V., Propagation and local behaviour of normally incident gravity waves over varying topography. *Eur. J. Mech. B: Fluids*, **11**, 213, 1992.

Rey, V., Belzons, M. and Guazzelli, E., Propagation of surface gravity waves over a rectangular submerged bar. *J. Fluid Mech.*, **235**, 453, 1992.

Young, I.R., Wave transformation over coastal reefs. *J. Geophys. Res.*, **94**, 9779-9789, 1989.